DOI: 10.1002/anie.201203711

Low-Coordinate Iron(I) and Manganese(I) Dimers: Kinetic Stabilization of an Exceptionally Short Fe–Fe Multiple Bond**

*Lea Fohlmeister, Shengsi Liu, Christian Schulten, Boujemaa Moubaraki, Andreas Stasch, John D. Cashion, Keith S. Murray, Laura Gagliardi, and Cameron Jones**

The fundamental and applied chemistry of metal–metal bonded complexes has rapidly expanded since Cotton's landmark report of metal–metal quadruple bonding in the dianion, $[Re_2Cl_8]^{2-}$, nearly 50 years ago.[1,2] Many of the recent advances in the field have centered on the stabilization of reactive low oxidation state/low coordination number M–M bonded complexes using sterically imposing ligand systems. Representative examples include the singly bonded zinc(I) and magnesium(I) dimers, [Cp*ZnZnCp*] (Cp* = C_5Me_5)[3] and $[(^{Dip}\text{Nacnac})\text{MgMg}(^{Dip}\text{Nacnac})]$ (^{Dip}Nacnac = $[(\text{DipNCMe})_2\text{CH}]$, Dip = 2,6-$i\text{Pr}_2\text{C}_6\text{H}_3$),[4] and the quintuply bonded chromium(I) dimer, [Ar′CrCrAr′] (Ar′ = 2,6-$(\text{Dip})_2\text{C}_6\text{H}_3$).[5] The unprecedented bonding in the latter initiated a number of studies aimed at preparing complexes with ever shorter Cr–Cr bonds.[6] These culminated in the isolation of quintuply bonded amidinate and guanidinate bridged complexes, for example, $[\text{Cr}_2\{\mu\text{-}N,N'\text{-}(\text{DipN})_2\text{CR}\}_2]$ (**1**; R = H, Me, or NMe_2), which exhibit the shortest known metal–metal bonds (ca. 1.74 Å).[7] As these bonds are essentially derived from the filling of five metal-based bonding molecular orbitals (MOs), the compounds are diamagnetic.

We have a strong background in developing bulky amidinate and guanidinate ligands for the stabilization of metal(I) dimers.[8] Most relevant to this study are the cobalt(I) and nickel(I) dimers, $[\text{M}_2\{\mu\text{-}N,N'\text{-}(\text{DipN})_2\text{CR}\}_2]$ (M = Co (**2**)[9] or Ni;[10] R = tBu, $\text{N}(\text{C}_6\text{H}_{11})_2$, or $\text{N}i\text{Pr}_2$), which are isostructural with **1**, and which, for M = Co, possess the shortest known Co–Co bonds (ca. 2.14 Å; for M = Ni, ca. 2.29 Å). However, unlike **1**, these more electron-rich systems are paramagnetic, and have lower M–M bond orders, owing to partial filling of metal-based anti-bonding MOs. We were keen to extend this study to the preparation of the corresponding iron(I) and manganese(I) dimers, as such compounds are unknown and have the potential to exhibit rare examples of multiple bonding between the metals, as well as M–M distances intermediate between those of **1** and **2**. We were especially interested in iron(I) dimers, as the current shortest known Fe–Fe bond (2.198 Å) exists in a related mixed valence amidinate bridged complex, $[\text{Fe}^{\text{I/II}}_2\{\mu\text{-}N,N'\text{-}(\text{PhN})_2\text{CPh}\}_3]$ (**3**),[11] which has a formal bond order of 1.5. It is of note that the Fe–Fe interaction in this high-spin complex ($S = 7/2$) is ferromagnetic in nature, as opposed to the more common antiferromagnetic interactions seen in related dimers, such as $[\text{Ar}'\text{Fe}^{\text{I}}\text{Fe}^{\text{I}}\text{Ar}']$ (**4**; Fe–Fe = 2.5151(9) Å, $S = 0$).[12–14] Furthermore, guanidinato/amidinato iron(I) complexes make attractive synthetic targets, as they will almost certainly be highly reactive species that have considerable potential for application in areas such as small molecule activations and enzyme mimicry. (compare with the well-developed chemistry of closely related, low-valent β-diketiminato iron complexes, such as $[\{(^{Dip}\text{Nacnac})\text{Fe}\}_2(\mu\text{-N}_2)]$).[15] Our preliminary efforts to prepare low coordinate, multiply bonded iron(I) and manganese(I) dimers are reported herein.

The reduction of $[\{(\text{Piso})\text{Fe}^{\text{II}}(\mu\text{-Br})\}_2]$ (Piso = $[(\text{DipN})_2\text{C}t\text{Bu}]$)[16] with the mild and soluble magnesium(I) reducing agent, $[\{(^{Mes}\text{Nacnac})\text{Mg}\}_2]$ (^{Mes}Nacnac = $[(\text{MesNCMe})_2\text{CH}]$, Mes = mesityl),[17] was initially carried out in cyclohexane under an argon atmosphere. Although this led to the desired iron(I) dimer, $[\text{Fe}^{\text{I}}_2(\mu\text{-}N,N'\text{-Piso})_2]$,[18] the complex was susceptible to disproportionation in solution and consistently co-crystallized with significant amounts (ca. 20 %) of the square-planar homoleptic complex, $[\text{Fe}^{\text{II}}(\kappa^2\text{-}N,N'\text{-Piso})_2]$.[19] This was found to be disordered over the same molecular site as the iron(I) dimer in the crystal lattice. As a result, reliable spectroscopic and crystallographic data could not be obtained for the compound. To overcome this problem, the bulkier guanidinato iron(II) precursor, $[\{(\text{Pipiso})\text{Fe}^{\text{II}}(\mu\text{-Br})\}_2]$ (Pipiso = $[(\text{DipN})_2\text{C}(cis\text{-2,6-Me}_2\text{NC}_5\text{H}_8)]$[20]), was prepared (see the Supporting Information) and reacted with one equivalent of $[\{(^{Mes}\text{Nacnac})\text{Mg}\}_2]$ to give the iron(I) dimer, $[\text{Fe}^{\text{I}}_2(\mu\text{-}N,N'\text{-Pipiso})_2]$ (**5**), in good yield (57 %), as a dark red-brown crystalline solid (Scheme 1). It is of note that all attempts to reduce $[\{(\text{Pipiso})\text{Fe}^{\text{II}}(\mu\text{-Br})\}_2]$ with more conventional reducing agents, such as elemental Mg or K, led to

---

[*] L. Fohlmeister, Dr. C. Schulten, Dr. B. Moubaraki, Dr. A. Stasch, Prof. K. S. Murray, Prof. C. Jones
School of Chemistry, Monash University
PO Box 23, Melbourne, VIC, 3800 (Australia)
E-mail: cameron.jones@monash.edu

S. Liu, Prof. L. Gagliardi
Department of Chemistry and
Minnesota Supercomputing Institute, University of Minnesota
207 Pleasant St, SE Minneapolis, MN-55455-0431 (USA)

Dr. J. D. Cashion
School of Physics, Monash University
PO Box 27, Melbourne, VIC, 3800 (Australia)

[**] We thank the Australian Research Council (C.J. and K.S.M.) and the U.S. Air Force Asian Office of Aerospace Research and Development (grant FA2386-11-1-4110 to C.J.). L.G. and S.L. thank the U.S. Department of Energy, Office of Basic Energy Sciences, Heavy Element Chemistry program for support (USDOE/DE-SC002183). The EPSRC is also thanked for access to the UK National Mass Spectrometry Facility. Nicholas Chilton (Monash) is thanked for carrying out D calculations.

Supporting information for this article, including details of the synthesis and characterization of all new compounds, and full details and references for the crystallographic and computational studies, is available on the WWW under http://dx.doi.org/10.1002/anie.201203711.

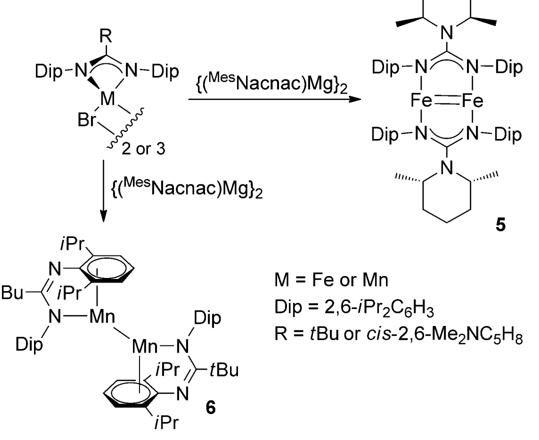

Scheme 1. Syntheses of compounds **5** and **6** (by-products omitted).

intractable product mixtures. While compound **5** is extremely air sensitive, it is stable in solution at room temperature for several days before signs of disproportionation are visible (namely, Fe metal deposition).

The molecular structure of **5** (Figure 1) shows it to be isostructural with **1** and **2**, in that the central $[Fe_2]^{2+}$ unit is bridged by two delocalized guanidinate ligands. Both Fe centers have T-shaped coordination geometries and the inner $Fe_2N_4C_2$ entity is essentially planar. The Fe–Fe distance of 2.1270(7) Å in **5** is shorter than all of the more than 7000 Fe–Fe interactions listed in the Cambridge Crystallographic Database,[21] and it is markedly shorter than the sum of two covalent radii for both low-spin iron (2.64 Å) and high-spin iron (3.04 Å).[22] No crystallographic or spectroscopic evidence was found for the presence of either bridging or terminal hydride ligands at the iron centers. These facts strongly suggest the presence of Fe–Fe multiple bonding in **5**.

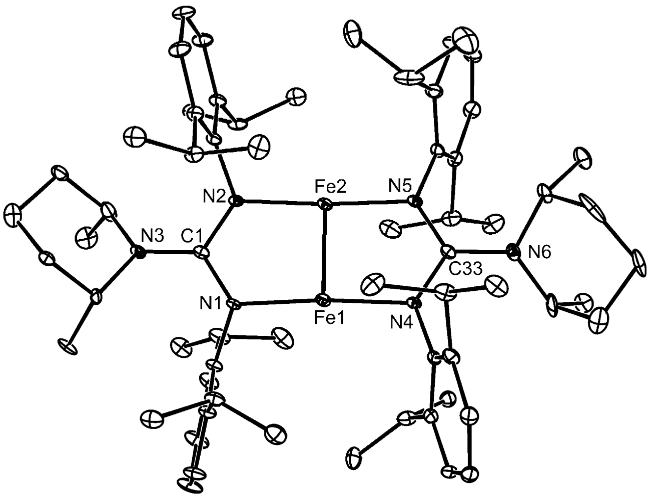

Figure 1. Molecular structure of **5** (25% thermal ellipsoids; hydrogen atoms omitted). Selected bond lengths (Å) and angles (°): Fe(1)–Fe(2) 2.1270(7), N(1)–Fe(1) 1.938(3), N(4)–Fe(1) 1.953(3), N(2)–Fe(2) 1.940(3), N(5)–Fe(2) 1.952(3), N(1)–C(1) 1.349(4), N(2)–C(1) 1.357(4), N(4)–C(33) 1.349(4), N(5)–C(33) 1.348(4), N(1)-C(1)-N(2) 114.7(3), N(4)-C(33)-N(5) 114.7(3), N(1)-Fe(1)-N(4) 175.46(12), N(2)-Fe(2)-N(5) 175.81(12).

The ^{1}H NMR spectra of **5** under argon atmosphere in solutions of $[D_6]$-benzene and $[D_{12}]$-cyclohexane are essentially identical and revealed the compound to be paramagnetic. When these solutions are exposed to a nitrogen atmosphere, their ^{1}H NMR spectra do not change. This suggests that the compound does not react with arene solvents or dinitrogen in solution at ambient temperature (compare with the formation of $[\{(Piso)Fe\}_2(\mu\text{-}N_2)]$ or $[(Piso)Fe(\eta^6\text{-toluene})]$ by the reduction of $[\{(Piso)Fe(\mu\text{-}Br)\}_2]$ in the presence of dinitrogen and/or toluene).[16] Similarly, the UV/Vis spectra of solutions of **5** in toluene and hexane are very similar, further indicating that the Fe–Fe bond of the complex is resistant to reaction with arenes.

The effective magnetic moment of **5** at room temperature ($[D_6]$-benzene, Evans method) was determined to be 8.1 μ_B, which is somewhat higher than the spin-only predictions for two non-interacting high-spin iron(I) centers ($\mu_{eff} = 5.48\,\mu_B$), and a high-spin, ferromagnetically coupled system with an $S = 3$ spin state ($\mu_{eff} = 6.93\,\mu_B$). Moreover, solid state magnetic susceptibility measurements of **5** (Figure 2) showed that its magnetic moment is largely independent of temperature between 300 and 150 K, remaining at 7.95 μ_B. It then decreases slowly to 6.3 μ_B at 8 K before rapidly decreasing to 3.3 μ_B at 2 K. In an attempt to gain information on the ground state spin, magnetization isotherms were determined at 2–20 K in fields of 0–5 T (Supporting Information, Figure S6). Saturation was not achieved at 2 K and high fields, with $M = 2.5\,N\mu_B$ at 2 K and 5 T, which is similar to the results recently obtained for the mixed-valence compound $[Fe^{I/II}{}_2\{\mu\text{-}N,N'\text{-}(PhN)_2CH\}_3]$ (saturated value for $S = 7/2$; $m_S = {}^1\!/_2$ lowest).[11b] The low M value signifies spin-orbit coupling, zero-field splitting, and orbital degeneracy contributions, whereas the lack of saturation reflects closely spaced energy levels relative to the ground level (see below). This likely leads to the high room temperature effective magnetic moment for **5**,[23] and although S could not be unambiguously determined through D value calculations on the compound, it is clear that the ground state has a significantly high spin value.

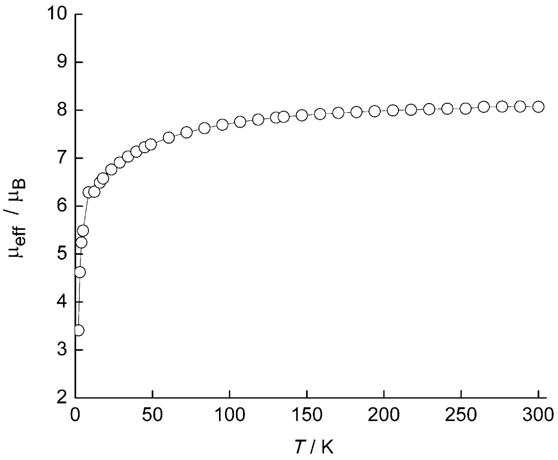

Figure 2. Plot of the effective magnetic moment versus temperature for dimer **5** in an applied field of 1 T. The solid line is a guide.

To shed further light on the oxidation state of the iron centers and the spin ground state of **5**, the Mössbauer spectrum of the compound was measured in zero applied field at 77 K (Figure S9). The dominant feature of the spectrum is a quadrupole doublet with an isomer shift (IS) of 0.44(1) $\mathrm{mm\,s^{-1}}$ and a large quadrupole splitting (QS) of 2.39(1) $\mathrm{mm\,s^{-1}}$. Although Mössbauer studies of high-spin iron(I) compounds are comparatively rare, it is clear from previous reports that the IS and QS values of such compounds can be very dependent upon the nature and symmetry of the surrounding ligands. Despite this, the Mössbauer data for **5** are similar to those for several β-diketiminato iron(I) compounds, for example, $[(^{t\mathrm{Bu}}\mathrm{Nacnac})\mathrm{Fe^{I}}(\eta^2\text{-HCCPh})]$ IS = 0.44(1) $\mathrm{mm\,s^{-1}}$, QS = 2.05(2) $\mathrm{mm\,s^{-1}}$ ($^{t\mathrm{Bu}}$Nacnac = $[(\mathrm{DipNC}t\text{-}\mathrm{Bu})_2\mathrm{CH}]$).[24] In contrast, the Mössbauer spectra of the related mixed-valence complex $[\mathrm{Fe^{I/II}}_2\{\mu\text{-}N,N'\text{-}(\mathrm{PhN})_2\mathrm{CH}\}_3]$ (both Fe centers are equivalent on the Mössbauer timescale)[11b] yield significantly different IS (0.65 $\mathrm{mm\,s^{-1}}$) and QS (0.32 $\mathrm{mm\,s^{-1}}$) values than those found for **5**. Although not unambiguous, the Mössbauer data for **5** are consistent with it possessing two high-spin iron(I) centers (see below).

DFT and multiconfigurational CASSCF/PT2 calculations (see the Supporting Information for full details) were carried out on a simplified model of **5**, $[\mathrm{Fe_2}\{\mu\text{-}N,N'\text{-}[(2,6\text{-}\mathrm{Me_2C_6H_3})\mathrm{N}]_2\mathrm{CNMe_2}\}_2]$ (**5a**), to gain further insight into its electronic structure and the nature of the very short Fe–Fe bond in the compound. Geometry optimizations (DFT) were initially carried out on **5a** in its quintet ($S = 2$) and septet ($S = 3$) spin states. The geometry of the latter spin state converged to be very close to that of **5** (with an Fe–Fe distance of 2.118 Å), while the former state optimized with a markedly shorter Fe–Fe bond (2.013 Å). Single point calculations revealed that the septet spin state is favored with respect to the quintet state by 6.5 $\mathrm{kcal\,mol^{-1}}$ (PT2) or 7.2 $\mathrm{kcal\,mol^{-1}}$ (DFT). Furthermore, the dominant electronic configuration for the septet state (62.3 %) yields a formal Fe–Fe bond order of two for **5a**. This can be understood when it is considered that, of the 14 metal-based valence electrons in the active space of the dimer (Figure S10), eight occupy four bonding MOs (σ-and π-type), four singly occupy anti-bonding MOs (σ* and π*-type), and two singly occupy essentially non-bonding orbitals (of δ and δ^* character). This gives rise to a bond order of two, and yields six unpaired electrons for the $S = 3$ spin state dimer. However, when partial occupancies of the CASSCF total ground state natural orbitals are taken into account, an effective bond order (EBO)[6b] of 1.19 is obtained (compared with an EBO of 1.29 for the $S = 2$ state). These values are greater than those for the mixed-valence system $[\mathrm{Fe^{I/II}}_2\{\mu\text{-}N,N'\text{-}(\mathrm{PhN})_2\mathrm{CH}\}_3]$, which has been reported as having a formal Fe–Fe bond order of 1.5 and an EBO of 1.15.[11b] As a result, it is reasonable to conclude that the exceptionally short Fe–Fe interaction in **5** is due to it possessing significant multiple bonding character between two high spin iron(I) centers. Moreover, a good agreement was found between the experimental Mössbauer IS and QS values for **5** (see above), and those calculated for **5a** ($S = 3$, IS = 0.41 $\mathrm{mm\,s^{-1}}$, QS = 2.04 $\mathrm{mm\,s^{-1}}$). These data provide further evidence for the proposed electronic structure of **5**.

The manganese(I) analogue of **5** was seen as an attractive synthetic target because of its potential reactivity, and because it could exhibit a metal–metal bond order (and length) between those of **1** and **5**. With the aim of accessing such a compound, attempts to prepare the dimeric manganese(II) precursor complex, $[\{(\mathrm{Pipiso})\mathrm{Mn^{II}}(\mu\text{-Br})\}_2]$, were made, though these were unsuccessful.[25] As a result, attention turned to the preparation (see the Supporting Information) and reduction of the related trinuclear complex, $[\{(\mathrm{Piso})\mathrm{Mn^{II}}(\mu\text{-Br})\}_3(\mathrm{THF})_2]$. Treatment of this complex with 1.5 equivalents of the magnesium(I) reagent $[\{(^{\mathrm{Mes}}\mathrm{Nacnac})\mathrm{Mg}\}_2]$ resulted in the formation of the $\mathrm{Mn^{I}}$ dimer **6** in moderate yield, as dark red-green dichroic crystals (Scheme 1). As a crystalline solid, compound **6** has negligible solubility in common organic solvents (such as, toluene, diethyl ether, and THF), which made the acquisition of meaningful solution spectroscopic data impossible.

Compound **6** is dimeric in the solid state (Figure 3) and contains an unsupported Mn–Mn interaction, the length of which (2.7170(9) Å) is indicative of a single bond (compare with 2.90 Å for $[\mathrm{Mn_2(CO)_{10}}]$).[26] Interestingly, the ligand has changed its coordination mode from N,N'-chelating in the precursor to what is best described as N-,η^3-arene-chelating in **6**. Moreover, the backbones of the Piso ligands in the dimer are largely electronically localized, and are therefore acting as imino-amides. Although carbonyl-free manganese(I) dimers are extremely rare, compound **6** is closely related to the β-diketiminato coordinated complex, $[\{(^{\mathrm{Dip}}\mathrm{Nacnac})\mathrm{Mn}\}_2]$ (**7**), though in that compound the ligands N,N'-chelate the metal centers.[27] The Mn–Mn bond length in **7** (2.721(1) Å) is essentially identical to that in **6**.

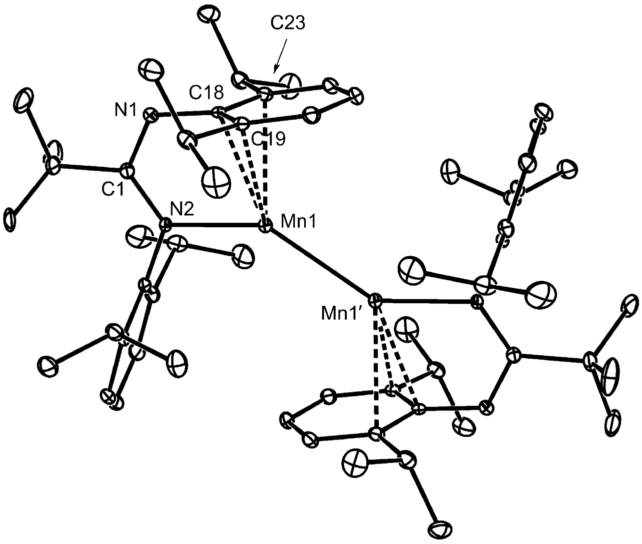

Figure 3. Molecular structure of **6** (25 % thermal ellipsoids; hydrogen atoms omitted). Selected bond lengths (Å) and angles (°): Mn(1)–Mn(2) 2.7170(9), Mn(1)–N(2) 2.076(12), C(1)–N(1) 1.308(4), C(1)–N(2) 1.356(4), Mn(1)–C(18) 2.509(3), Mn(1)–C(19) 2.710(3), Mn(1)–C(23) 2.766(3), N(1)-C(1)-N(2) 121.7(2), Mn(1)′-Mn(1)-N(2) 143.42(7). Symmetry operation: ′$-x+1$, $-y+2$, $-z+1$.

The magnetic susceptibility of compound **6** in the solid state was measured at 2–300 K (Figure 4) and the room temperature effective magnetic moment was found to be 4.39 μ_B per dimer. This suggests a high spin state for the manganese(I) ions ($3d^54s^1$ or $3d^6$), but the significantly lower experimental value compared to the spin-only value for two non-interacting manganese(I) ions ($3d^54s^1$: 9.80 μ_B or $3d^6$: 6.93 μ_B) is indicative of antiferromagnetic coupling between the metal centers, with a Curie temperature (T_c) significantly higher than 300 K. The decrease of χ from 300 K to 15 K points to an $S=0$ coupled ground state at 0 K for the dimer, even though χ increases again below 15 K, presumably due to the unavoidable presence of a small amount of paramagnetic impurity. A good fit to an $S=5/2$ (per Mn) Heisenberg model ($-2\,J\mathbf{S}_1.\mathbf{S}_2$) gave parameters: $g=2.00$, $J=-40.2\ \mathrm{cm}^{-1}$ (fraction monomer 0.002). Use of an $S=2$ (per Mn) model gave similar parameters (see the Supporting Information), as the $S=0$, 1, and 2 coupled states are the only ones thermally populated up to 300 K. It is of note that the related Mn^{I} dimer **7** showed broadly similar magnetic behavior to **6**.[27]

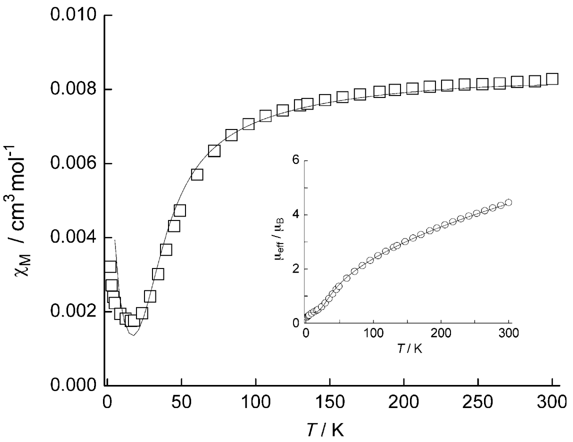

Figure 4. The temperature dependence (2–300 K) of the magnetic susceptibility (main plot) and effective magnetic moment (insert plot) of **6** (per dimer). The solid line (main plot) is that calculated for an $S=5/2{:}5/2$ dimer model using the parameters given in the text.

Geometry optimizations (DFT) carried out on a simplified model of **6**, $[\{\{t\mathrm{BuC}[(2,6\text{-}\mathrm{Me}_2\mathrm{C}_6\mathrm{H}_3)\mathrm{N}]_2\}\mathrm{Mn}\}_2]$ (**6a**), showed that only the geometry of the $S=5$ spin state converged (Mn–Mn = 2.741 Å) close to the solid state geometry of **6**. A multiconfigurational analysis of **6a** ($S=5$) revealed a single dominating electronic configuration (95.5 %) and an EBO of 0.42 for the Mn–Mn interaction. From the results of previous studies,[6b,11b] it is not surprising that this measure of bond order provides a value less than unity, and it is clear that there is a significant Mn–Mn interaction in **6a**. The natural bond orbitals for the compound show that its unpaired electrons are essentially localized in the metal-centered 3d orbitals, while the Mn 4s electrons are involved in forming a single bond between the manganese centers (Figure S11). On the basis of these calculations, the best interpretation of the results from the magnetic measurements on **6** is that there is antiferromagnetic coupling between two $S_1=S_2=5/2$ spin centers, very similar to that described for **7**.

In conclusion, a bulky guanidinato-stabilized iron(I) dimer, with the shortest Fe–Fe bond reported to date, has been prepared and shown by magnetic, Mössbauer, and computational studies to contain two high-spin iron(I) centers that display significant multiple-bond character. A related antiferromagnetically coupled manganese(I) dimer, containing a rare example of an unsupported, carbonyl free Mn–Mn single bond, has also been synthesized and fully characterized. Investigations into the utility of these highly reactive compounds as reagents for small molecule activations are underway in our laboratory.

Received: May 14, 2012
Revised: June 14, 2012

Keywords: density functional calculations · iron · magnesium · manganese · metal-metal interactions

---

[1] F. A. Cotton, L. A. Murillo, R. A. Walton, *Multiple Bonds Between Metal Atoms, 3rd ed.*, Springer, Berlin, **2005**.

[2] F. A. Cotton, N. F. Curtis, B. F. J. Johnson, J. T. Mague, J. S. Wood, C. B. Harris, W. R. Robinson, S. J. Lippard, *Science* **1964**, *145*, 1305–1307.

[3] I. Resa, E. Carmona, E. Gutierrez-Puebla, A. Monge, *Science* **2004**, *305*, 1136–1138.

[4] S. P. Green, C. Jones, A. Stasch, *Science* **2007**, *318*, 1754–1757.

[5] T. Nguyen, A. D. Sutton, M. Brynda, J. C. Fettinger, G. J. Long, P. P. Power, *Science* **2005**, *310*, 844–847.

[6] a) F. R. Wagner, A. Noor, R. Kempe, *Nat. Chem.* **2009**, *1*, 529–536; b) M. Brynda, L. Gagliardi, B. O. Roos, *Chem. Phys. Lett.* **2009**, *471*, 1–10.

[7] a) C.-W. Hsu, J.-S. K. Yu, C.-H. Yen, G.-H. Lee, Y.-C. Tsai, *Angew. Chem.* **2008**, *120*, 10081–10084; *Angew. Chem. Int. Ed.* **2008**, *47*, 9933–9936; b) A. Noor, G. Glatz, R. Müller, M. Kaupp, S. Demeshko, R. Kempe, *Z. Anorg. Allg. Chem.* **2009**, *635*, 1149–1152.

[8] C. Jones, *Coord. Chem. Rev.* **2010**, *254*, 1273–1289.

[9] a) C. Jones, C. Schulten, R. P. Rose, A. Stasch, S. Aldridge, W. D. Woodul, K. S. Murray, B. Moubaraki, M. Brynda, G. La Macchia, L. Gagliardi, *Angew. Chem.* **2009**, *121*, 7542–7546; *Angew. Chem. Int. Ed.* **2009**, *48*, 7406–7410; b) for related rhodium(I) chemistry, see: C. Jones, D. P. Mills, A. Stasch, *Dalton Trans.* **2008**, 4799–4804.

[10] C. Jones, C. Schulten, L. Fohlmeister, A. Stasch, K. S. Murray, B. Moubaraki, S. Kohl, M. Z. Ertem, L. Gaglaiardi, C. J. Cramer, *Chem. Eur. J.* **2011**, *17*, 1294–1303.

[11] a) F. A. Cotton, L. M. Daniels, L. R. Falvello, J. H. Matonic, C. A. Murillo, *Inorg. Chim. Acta* **1997**, *256*, 269–275; b) for a recent comprehensive spectroscopic and computational analysis of the closely related complex, $[\mathrm{Fe}^{\mathrm{I/II}}{}_2\{\mu\text{-}N,N'\text{-}(\mathrm{PhN})_2\mathrm{CH}\}_3]$, see: C. M. Zall, D. Zherebetskyy, A. L. Dzubak, E. Bill, L. Gagliardi, C. C. Lu, *Inorg. Chem.* **2012**, *51*, 728–736.

[12] T. Nguyen, W. A. Merrill, C. Ni, H. Lei, J. C. Fettinger, B. D. Ellis, G. J. Long, M. Brynda, P. P. Power, *Angew. Chem.* **2008**, *120*, 9255–9257; *Angew. Chem. Int. Ed.* **2008**, *47*, 9115–9117.

[13] For examples of paramagnetic compounds with Fe–Fe bonds, see: a) H. Lei, J.-G. Guo, J. C. Fettinger, S. Nagase, P. P. Power, *J. Am. Chem. Soc.* **2010**, *132*, 17399–17401; b) C. R. Hess, T. Weyhermüller, E. Bill, K. Wieghardt, *Angew. Chem.* **2009**, *121*, 3758–3761; *Angew. Chem. Int. Ed.* **2009**, *48*, 3703–3706; c) A. Klose, E. Solari, C. Floriani, A. Chiesi-Villa, C. Rizzoli, N. Re, *J.*

Am. Chem. Soc. **1994**, *116*, 9123–9135; d) F. A. Cotton, L. M. Daniels, J. H. Matonic, C. A. Murillo, *Inorg. Chim. Acta* **1997**, *256*, 277–282.

[14] For a discussion on ferromagnetic Fe–Fe interactions, see G. H. Timmer, J. H. Berry, *C. R. Chim.* **2012**, *15*, 192–201.

[15] a) P. L. Holland, *Acc. Chem. Res.* **2008**, *41*, 905–914; b) M. M. Rodriguez, E. Bill, W. W. Brennessel, P. L. Holland, *Science* **2011**, *334*, 780–783.

[16] R. P. Rose, C. Jones, C. Schulten, S. Aldridge, A. Stasch, *Chem. Eur. J.* **2008**, *14*, 8477–8480.

[17] a) A. Stasch, C. Jones, *Dalton Trans.* **2011**, *40*, 5659–5672; b) S. J. Bonyhady, C. Jones, S. Nembenna, A. Stasch, A. J. Edwards, G. J. McIntyre, *Chem. Eur. J.* **2010**, *16*, 938–955.

[18] From one reduction a low yield of the C–H activated product, $[(\text{Piso}^{-\text{H}})\text{Fe}^{\text{II}}(\mu\text{-H})\text{Mg}(\text{THF})(^{\text{Mes}}\text{Nacnac})]$ ($\text{Piso}^{-\text{H}} = \text{DipNC}(t\text{Bu})\text{N}\{2\text{-}i\text{Pr-6-}[\text{C(H)(Me)(CH}_2)]\text{-C}_6\text{H}_3\}$), was obtained. See the Supporting Information for details of the crystal structure and formation of this compound.

[19] $\text{Fe}^{\text{II}}(\kappa^2\text{-}N,N'\text{-Piso})_2$] was subsequently intentionally synthesized and fully characterized (see the Supporting Information). Closely related square planar bis(amidinato)-iron(II) complexes have been reported. C. A. Nijhuis, E. Jellema, T. J. J. Sciarone, A. Meetsma, P. H. M. Budzelaar, B. Hessen, *Eur. J. Inorg. Chem.* **2005**, 2089–2099.

[20] G. Jin, C, Jones, P. C. Junk, K.-A. Lippert, R. P. Rose, A. Stasch, *New J. Chem.* **2009**, *33*, 64–75.

[21] As determined by a survey of the Cambridge Crystallographic Database, May, **2012**.

[22] B. Cordero, V. Gomez, A. E. Platero-Prats, M. Reves, J. Echeverria, E. Cremades, F. Barragan, S. Alvarez, *Dalton Trans.* **2008**, 2832–2838.

[23] To rule out significant contributions from paramagnetic impurities to the room temperature effective magnetic moment of **5**, the field dependency (at 0.01, 0.1, and 1 T) of μ_{eff} for the compound was examined (Supporting Information, Figure S7). A small field dependency was observed below 70 K, thus indicating the presence of a small amount of impurity. This is unavoidable for such an air-sensitive compound. However, in the temperature range of 150–300 K, the experiments pointed to a negligible contribution from the impurity to the value of μ_{eff} for **5**.

[24] S. A. Stoian, Y. Yu, J. M. Smith, P. L. Holland, E. L. Bominaar, E. Münck, *Inorg. Chem.* **2005**, *44*, 4915–4922.

[25] The related guanidinato complexes, $[\{(\text{Giso})\text{Mn}^{\text{II}}(\mu\text{-X})_2\}_2]$ ($\text{Giso} = [(\text{DipN})_2\text{CN}(\text{C}_6\text{H}_{11})_2]$, X = Cl or Br) were prepared (see the Supporting Information), but their reductions gave complex product mixtures.

[26] R. Bianchi, G. Gervasio, D. Marabello, *Inorg. Chem.* **2000**, *39*, 2360–2366.

[27] J. Chai, H. Zhu, C. Stückl, H. W. Roesky, J. Magull, A. Bencini, A. Caneschi, D. Gatteschi, *J. Am. Chem. Soc.* **2005**, *127*, 9201–9206. See also, the dianionic Mn^{I} dimer, $[\text{Mn}_2\{(\text{NDip})_2\text{SiMe}_2\}_2]^{2-}$ (Mn–Mn: 2.78198 Å): D.-Y. Lu, J.-S. Yu, T.-S. Kuo, G.-H. Lee, Y. Wang, Y.-C. Tsai, *Angew. Chem.* **2011**, *123*, 7753–7757; *Angew. Chem. Int. Ed.* **2011**, *50*, 7611–7615.

Communications

Metal–Metal Bonds

L. Fohlmeister, S. Liu, C. Schulten,
B. Moubaraki, A. Stasch, J. D. Cashion,
K. S. Murray, L. Gagliardi,
C. Jones* ____________ ■■■■–■■■■

Low-Coordinate Iron(I) and Manganese(I) Dimers: Kinetic Stabilization of an Exceptionally Short Fe—Fe Multiple Bond

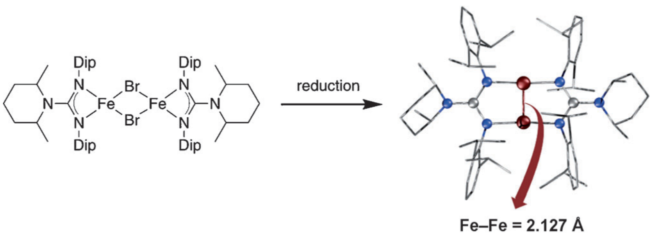

Not just any old iron! The reduction of a bulky guanidinato iron(II) bromide complex yields a three-coordinate iron(I) dimer that possesses the shortest Fe–Fe interaction (2.127 Å) reported to date. Magnetic, Mössbauer, and computational studies show the unprecedented compound to contain two high-spin iron(I) centers with significant multiple-bond character. A related dimer containing a rare example of an unsupported, carbonyl-free Mn—Mn bond is also described.